



Contents lists available at ScienceDirect

Microchemical Journal

journal homepage: [www.elsevier.com/locate/microc](http://www.elsevier.com/locate/microc)

# Mycenaean glass from the Argolid, Peloponnese, Greece: A technological and provenance study



N. Zacharias<sup>a,\*</sup>, M. Kaparou<sup>a,b</sup>, A. Oikonomou<sup>a,c</sup>, Zs. Kasztovszky<sup>d</sup>

<sup>a</sup> Department of History, Archaeology and Cultural Resources Management, University of the Peloponnese, 24133 Kalamata, Greece

<sup>b</sup> N.C.S.R. Demokritos, 15 310 Ag. Paraskevi, Attiki, Greece

<sup>c</sup> Department of Archaeology, University of Nottingham, NG72RD Nottingham, UK

<sup>d</sup> Nuclear Analysis and Radiography Department MTA, Centre for Energy Research, H-1121 Budapest, Konkoly Thege 29-33, Hungary

## ABSTRACT

Major glass-technology achievements and the spread of glass artifacts are mostly outlined in the archaeological record between the 16th and 12th c. BCE with its advances being linked to Mesopotamia and Egypt (Henderson, 2013 [1]). During the Late Bronze Age, Peloponnese is acknowledged as a major area of the Mycenaean world witnessed by the wealth and ubiquity of its material culture. Within the framework of a large research program, glass collections from 16th–13th c. BCE Late Bronze Age/Mycenaean sites in NE Peloponnese, Greece, have been studied analytically and tailored to address issues related to questions such as, whether glass was imported in the form of ingots and/or previously shaped artifacts via exchange routes or produced in local glassmaking workshops. A first study of the collection towards its state of preservation and provenance assignments was presented in Zacharias et al. (2013) [2].

The aim of this paper is to identify the technology and source of the primary glass used and, thus, to appoint the Mycenaean glass industry of Argolid within the broader Mycenaean, Mediterranean network and further Egypt and Mesopotamia.

The study resulted in the chemical fingerprinting of the collection with the use of the totally non-invasive techniques of Optical Microscopy (OM), X-Ray Fluorescence (XRF), Prompt Gamma Activation Analysis (PGAA) and Scanning Electron Microscopy coupled with an Energy Dispersive X-Ray Analyser - (SEM/EDS) in quasi invasive mode. The statistical analyses provided technological evidence for compositional similarities among the samples that form two major compositional groups, with at least the one associated with artifacts originating from Egypt. Regarding their coloration at least two cobalt colorants can be identified with respect to the cobalt-associated impurities.

## 1. Introduction

From the onset of the Late Bronze Age - LHI and LHII - the geographic center of the Mycenaean world is set in central Greece with Argolid preponderating among other prominent areas such as Messenia, Laconia, Attica, Boeotia, Eastern Fokis and coastal Thessaly [3] (for the corresponding chronology see Appendix, Table 1).

During the Mycenaean Palatial Period - LHIIIA and LHIIIB - local power centers emerge holding administrative and religious control with parallel wending of production, trade and storage of goods, with the archaeological data reinforcing the image of a well-ranked society [4]. This is particularly clear in palaces, such as Mycenae, Tiryns, Pylos and Thebes.

Argolid, with three citadels, at least two impressive palaces,

elaborate royal tombs and many fortified hills, appears to be the dominating center, with perhaps only Boeotia with the palace of Thebes yielding evidence of similar significance. This is also apparent from the archaeological evidence with respect to the Mycenaean cultural impact, which reaches the coast of Asia Minor and Northern Greece, while evidence of trade relations links the region with Cyprus, the Near East, the Central Mediterranean and the Balkans.

In the present study, samples from four locations in Argolid are studied, namely Palaia Epidavros, Mycenae, Kazarma and Ancient Asine [5–7] - (see Appendix-Table 2).

## 2. Objectives

In the field of archaeometry, the number of glass studies is indeed

\* Corresponding author.

E-mail address: [zacharias@uop.gr](mailto:zacharias@uop.gr) (N. Zacharias).

**Table 1**

Evaluation of the accuracy and precision of SEM/EDS, XRF and PGAA analyses (c.v.: certified values); values are given in wt%; n.d. stands for not detected.

	NIST 620 c.v.	NIST 621 c.v.	NIST 620 SEM/EDX	NIST 621 SEM/EDX	NIST 620 XRF	NIST 621 XRF	NIST 620 PGAA	NIST 621 PGAA
SiO <sub>2</sub>	72.08 ± 0.08	71.13 ± 0.03	71.14 ± 1.8	70.89 ± 1.9	71.87 ± 2.1	72.01 ± 2.4	71.5 ± 0.5	71.0 ± 0.5
Na <sub>2</sub> O	14.39 ± 0.06	12.74 ± 0.05	14.01 ± 1.5	12.11 ± 1.3	13.99 ± 1.2	13.01 ± 0.1.3	14.6 ± 0.3	12.7 ± 0.2
CaO	7.11 ± 0.05	10.71 ± 0.05	7.27 ± 0.8	11.11 ± 1.9	7.02 ± 0.7	10.09 ± 1.1	7.1 ± 0.2	10.5 ± 0.3
MgO	3.69 ± 0.05	0.27 ± 0.03	3.81 ± 0.3	0.32 ± 0.02	3.55 ± 0.4	0.19 ± 0.1	3.8 ± 0.2	0.3 ± 0.0
Al <sub>2</sub> O <sub>3</sub>	1.80 ± 0.03	2.76 ± 0.04	1.67 ± 0.14	2.59 ± 0.23	1.69 ± 0.2	2.93 ± 0.4	1.9 ± 0.1	2.85 ± 0.1
K <sub>2</sub> O	0.41 ± 0.03	2.01 ± 0.03	0.51 ± 0.04	1.95 ± 0.12	0.39 ± 0.03	1.96 ± 0.18	0.40 ± 0.01	2.04 ± 0.04
SO <sub>3</sub>	0.28 ± 0.02	0.13 ± 0.02	0.21 ± 0.03	0.11 ± 0.02	0.21 ± 0.03	0.18 ± 0.03	0.30 ± 0.01	0.16 ± 0.01
BaO	n.d.	0.12 ± 0.05	0.11 ± 0.01	0.12 ± 0.01	0.11 ± 0.04	0.11 ± 0.02	n.d.	0.17 ± 0.02
As <sub>2</sub> O <sub>3</sub>	0.056 ± 0.003	0.03 ± 0.001	0.049 ± 0.001	0.03 ± 0.001	0.065 ± 0.008	0.039 ± 0.003	0.07 ± 0.01	0.04 ± 0.01
Fe <sub>2</sub> O <sub>3</sub>	0.043 ± 0.004	0.04 ± 0.001	0.041 ± 0.001	0.048 ± 0.001	0.032 ± 0.005	0.039 ± 0.004	0.046 ± 0.003	0.014 ± 0.001
TiO <sub>2</sub>	0.018 ± 0.002	0.003 ± 0.0003	0.011 ± 0.001	0.002 ± 0.0001	0.014 ± 0.002	0.029 ± 0.003	0.017 ± 0.001	0.014 ± 0.001

inversely analogous to the wealth of finds that come to light. Therefore, the present study aims to contribute to the relatively restricted body of data related to the era under study. What is more, it aims to acknowledge the assemblages from the specific sites outlined previously.

The application of a wide range of non-destructive or of minimal intervention techniques was selected, in an attempt to secure the analytical range and extract the most information available. Via these, additionally, the study aimed to study and assess the technological level during the study period, in order to enlighten a part of the cultural material of the studied area. This was partly addressed by pinpointing the main raw materials and methods used for the formation of these specific samples. Furthermore, within the objectives lied the clustering of samples produced with the same technology by forming groups sharing similar chemical characteristics. This might yield data towards addressing questions related to provenance issues and trading routes and possibly appointing the glass production of the sites under study to the Egyptian or/and Mesopotamian established production context, according to their unique chemical fingerprint.

Finally, the archaeological and bibliographic data hitherto clearly demonstrate the existence of secondary production in the Mycenaean world, while the verification of the existence of primary production is still a challenging objective in archaeological research. The evaluation of a craft as a primary or secondary one using all available data - archaeological, bibliographic and technological - is an important objective of research in the study of any local Mycenaean glass craft industry. Though difficult to address in this case - in the absence of glass working and/or making debris and archaeological/bibliographic data-, the analytical data aspire to contribute to our overall knowledge with respect to this challenging issue.

### 3. Materials

In the present study, 30 glass samples excavated at Palaia Epidavros (PE), Mycenae (M), ancient Asine (AA) and Kazarma (K) were investigated scientifically (see Appendix, Tables 2–3).

The samples are divided, as expected, in two broad categories, in the characteristic Mycenaean relief plaques and in spherical or round beads, exhibiting a rather tight variation in color. Most of the samples have the characteristic deep blue color, while there is one sample having turquoise and four of violet color. The samples derive from burial contexts and they date between 1600 and 1060 BCE forming two broad categories: Early Helladic (c. 1600–1300 BCE) and Late Helladic (c. 1300–1100 BCE) (see Appendix, Table 1).

### 4. Methods

The samples were documented and in situ photos were taken at each area's storehouse. In an attempt to secure optimum analysis by means of SEM/EDS, a small chunk was removed from each sample and polishing of the selected surface area occurred. Then, further polishing of the

abraded glass surface with garnet paper of various grits (1000, 1200, and 1500 grits) took place. The chunks were then cleaned in purified water and embedded in epoxy-resin. Finally, they were carbon coated.

The instrumentation applied on the assemblage entailed a light transmission optical lenses system (LED)-OM, SEM, XRF and at a next step PGAA analysis.

The portable OM of the model i-Scope-Moritex uses LED connected to a laptop for digital registration and photos management. The use of magnifying lenses ×15, ×50 (and of polarized light) and ×200 allowed the micro photography of distinct phases and characteristics in an attempt to assess the preservation state of the artifacts, aiding effective sampling and highlighting some technological characteristics.

SEM was the principal tool of analysis. A FEI (model Inspect) set up was used; the voltage applied on the filament was 25 kV and every spectrum was collected for 250 live s. The fluorescence X-rays were detected through a SUTW Si(Li) spectrometer placed at 35° with respect to the sample surface. The SEM used was combined with EDS analysis; internal correction software that corrects against matrix effects (ZAF) was used for analytical data calibration [8]. An in-length presentation of the above set-up is given at Oikonomou et al. [9].

A milliprobe XRF spectrometer was employed at two high-voltage settings: a low-energy excitation mode without the employment of a filter (high voltage set at 15 kV) which addressed the analysis of all major and minor elements heavier than magnesium ( $Z > 12$ ), whereas the use of a filter at a high energy excitation mode (high voltage set at 40 kV) enabled the detection of elements from  $Z > 19$  including minor and trace elements. Subsequently, the quantification was realised on the basis of the Fundamental Parameter (FP) method by means of an in-house (N.C.S.R. "Demokritos") developed software. The above set-up has been described extensively in the literature [10,11].

Glass standards (Corning and NIST) are periodically used to check the performance of the system [12]. The accuracy and precision of the quantitative analysis both by means of SEM and by means of XRF was deemed satisfactory, after setting against the analysis of certified reference glasses, such as NIST 620 and NIST 621 (Table 1).

On a small number of artifacts for which even micro-sampling was not allowed due to their complete form, the totally non-invasive PGAA technique was selected, since the analytical information the technique monitors is of the glass matrix with no interference from the surface. Furthermore, it offered the identification of few trace elements. PGAA is a non-destructive bulk analytical method, based on the detection of characteristic gamma photons, emitted in ( $n,\gamma$ ) reactions [13]. For PGAA, we use an external cold neutron beam of  $9.6 \times 10^7 \text{ cm}^{-2}\text{s}^{-1}$ , guided away from the Budapest Research Reactor [14]. The prompt gamma spectra were collected by Compton-suppressed HPGe detector, which has been precisely calibrated. The gamma-ray spectra were evaluated using the Hypermet-PC program [15]. The quantitative analysis is based on the  $k_0$  principle, using the spectroscopic data libraries developed at the laboratory. The composition was determined using the methods described by Révay in 2009 [16]. For the

determination of boron a separate routine was used [17]. The most significant advantage of PGAA is that it does not require sampling or any preparation of archaeological objects. As a consequence of PGAA investigations, neither any destruction nor significant induced radioactivity is produced. PGAA has been applied successfully in characterisation of archaeological stone objects [18], as well as for glass [19,12].

## 5. Results and discussion

### 5.1. Weathering patterns/technological observations

Surface examination can characterize corrosion patterns, to assess weathering effects from the burial environment, but also, importantly, to provide valuable technological data [20]. The use of OM yielded useful information on the distinct phases of the material under study. In the examples presented, various corrosion phenomena were observed readily with the aid of solely the LED facility. Overall, glasses with greater surface width have been shown to exhibit logarithmically accelerated corrosion [21], a fact difficult to estimate in glass beads and plaques which are generally of small dimensions.

The most common observation which was made in the overwhelming majority of the samples was micro-pitting with characteristic concentric weathering layers around the areas of healthy glass which form a local crust of a varying thickness 1–2 mm for samples exhibiting light corrosion and > 3 mm for the heavily weathered ones. Fig. 1 (a) shows a typical example of light corrosion with extended areas of surviving glass surrounding concentric layers of degradation. In Fig. 1 (b–c) iridescence interference between rays of light reflected from thin alternating air layers which occur on the silica-rich glasses are formed, due to the loss of alkalis and weathered glass crusts are formed in the glass. The layers are formed in fluctuating environmental conditions, where corrosion occurs in distinct phases [22].

In Fig. 1 (d), air bubbles characteristic of technological information pointing to the method of manufacture were observed. Furthermore, there are indications of glass dissolution/recrystallization patterns

(lower part of the photo). The exhibition of a preferred orientation of the bubbles could be an indication of the use of the wire winding technique in fashioning the beads, along with the fact that the perforations of the beads were performed with precision suggesting their formation on a wire or a reed. The small dimensions of the objects would allow for heating in an open fire too.

The formation of the relief plaques would have been performed with the use of simple open molds, as suggested by their typological study. The detection of marks of excess glass removal in some samples is probably an indication of the glass being hot, when entering the mold. Some samples have their back side slightly bending and with somewhat rounded ends, which could suggest the glass property of contracting when heated (Fig. 2 (a)). The glossy surface noted in other examples could be indicating the glass removal from the mold, when still retaining some heat (Fig. 2 (b)).

### 5.2. Analytical results

#### 5.2.1. PGAA results

The data obtained by means of the PGAA analysis were set against the data obtained from the principal tool of analysis, namely SEM, and the results provided by XRF in order to assess the precision of the instrumentation applied. Fifteen samples from Argolid - and from assemblages not presented herein - were analyzed via PGAA, having been studied formerly with SEM and XRF. It is of relevant importance to underline that the PGAA data represent the glass matrix avoiding surface information. The correspondence between the different settings was satisfactory, rendering the already obtained analyses via the other tools secure and highlighting the effectiveness of PGAA for glass studies. It is interesting, though, that the cobalt oxide detected by means of PGAA was not detected by means of XRF. Examples are presented in Table 2a–b.

5.2.1.1. *Silica.* The alumina levels detected are plotted against the silica levels in an attempt to identify the source of silica (Fig. 3). Three

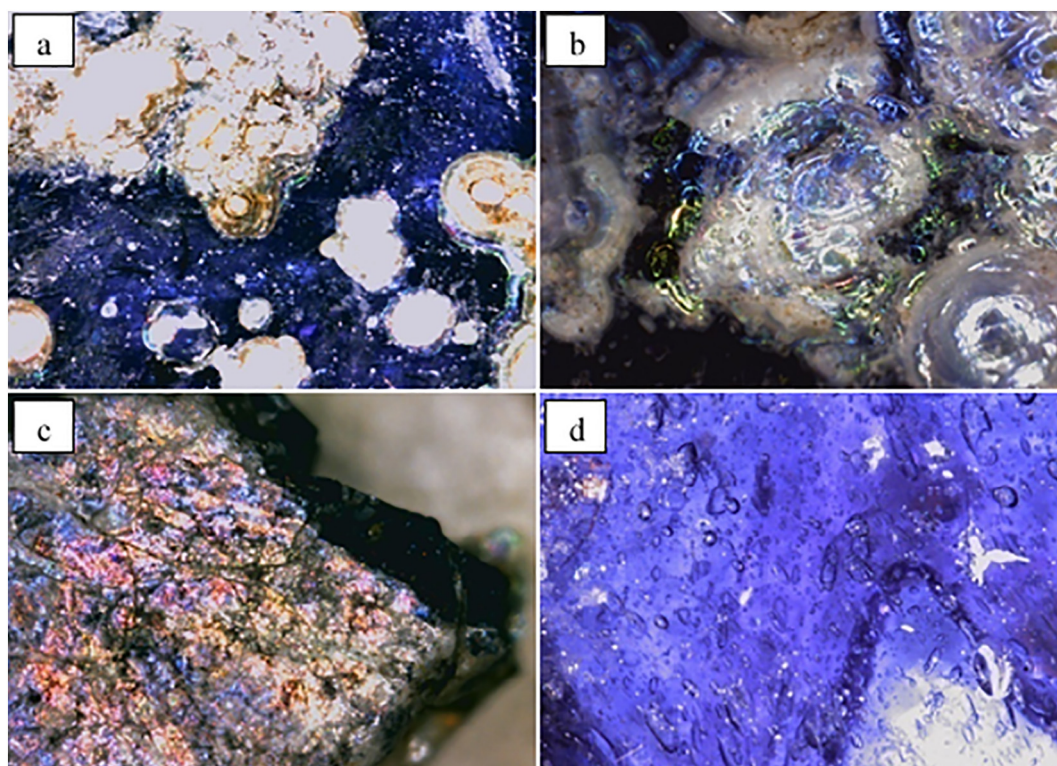


Fig. 1. (a) PE25/magnification  $\times 50$ . (b) PE32/magnification  $\times 50$ . (c) PE24/magnification  $\times 50$ . (d) PE33/magnification  $\times 50$ .



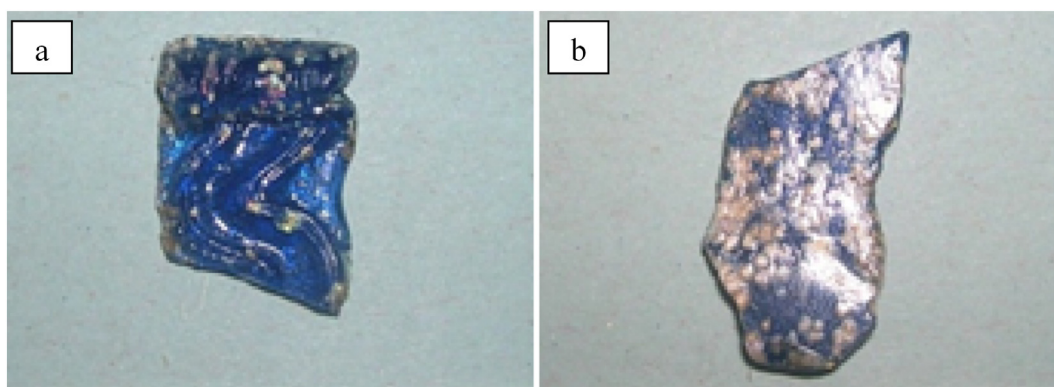


Fig. 2. (a) PE32. (b) PE33.

major groups are defined. The first with alumina < 1.00 wt%, a second one with alumina levels varying between 1.5 and 3 wt% and a third group with alumina above 3.00 wt%. The samples from Palaia Epidavros and Kazarma generally correspond to Mycenaean published parallels with respect to their alumina content [20–23]. One sample from Mycenae and the sample from ancient Asine exhibit higher in comparison to the latter group's alumina levels, but the trend is clearly different for the rest of the samples from Mycenae which exhibit interestingly high alumina levels.

The low alumina group must have been manufactured using quartz pebbles, rather than sand as the main silica source. Opting for quartz is reflected in the glass batch in the lower impurity levels, since it is a purer source of silica, and, therefore, it was typically selected by the glassmakers of the period. Five samples fall in this grouping, four of which are of violet color and two of deep blue, possibly having been made by a purer colorant source, which would not yield additional alumina to the batch. The majority of samples shows an excess of alumina with a mean value of around 2.00 wt%. It is suggested that most

Table 2

a. Comparison between PGAA, SEM/EDS and XRF analytical data.

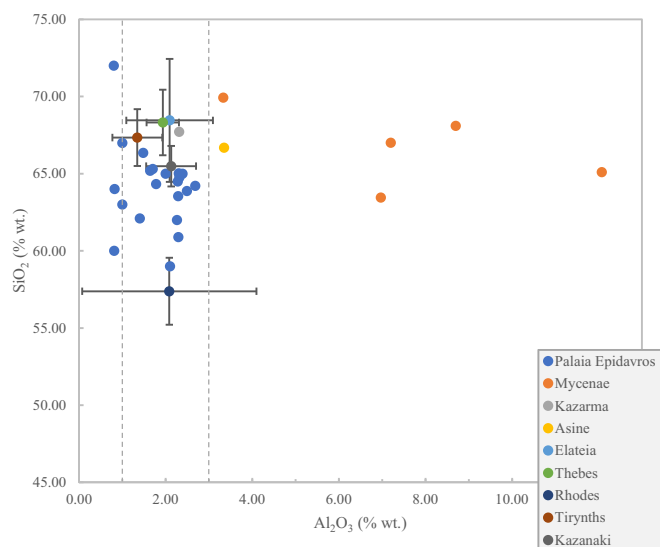
b. The SEM/EDX and XRF results are presented in Table 4 (see Appendix).

	PE24		PE26	
	PGAA c% ± unc. (ox/ox)	SEM (wt%)	PGAA c% ± unc. (ox/ox)	SEM (wt%)
P	n.d.	0.23 ± 0.2	n.d.	0.21 ± 0.40
H <sub>2</sub> O	3.08 ± 0.06	n.d.	3.35 ± 0.05	n.d.
Na <sub>2</sub> O	16.00 ± 0.3	15.92 ± 2.4	15.7 ± 0.3	18.85 ± 2.90
MgO	3.52 ± 0.2	3.51 ± 0.5	4.07 ± 0.2	3.43 ± 0.51
Al <sub>2</sub> O <sub>3</sub>	1.92 ± 0.08	2.33 ± 4	2.28 ± 0.09	2.29 ± 0.60
SiO <sub>2</sub>	64 ± 0.6	64.96 ± 1.00	64 ± 0.6	63.54 ± 0.99
K <sub>2</sub> O	2.27 ± 0.05	2.49	2.13 ± 0.04	1.98 ± 0.6
CaO	6.47 ± 0.2	6.19	6.27 ± 0.2	6.74 ± 1.2

	PGAA	XRF (wt%)	PGAA	XRF (wt%)
SO <sub>4</sub>	n.d.	0.49 ± 0.09	n.d.	n.d.
Cr <sub>2</sub> O <sub>3</sub>	n.d.	0.40 ± 0.01	n.d.	n.d.
ZnO	n.d.	0.18 ± 0.06	n.d.	n.d.
PbO	n.d.	n.d.	n.d.	n.d.
SnO	n.d.	n.d.	n.d.	n.d.
TiO <sub>2</sub>	0.09 ± 0.004	0.11 ± 0.05	0.09 ± 0.004	n.d.
MnO	0.12 ± 0.004	0.24 ± 0.06	0.13 ± 0.005	n.d.
Fe <sub>2</sub> O <sub>3</sub>	0.61 ± 0.03	0.73 ± 0.06	0.66 ± 0.03	0.9 ± 0.08
CoO	0.11 ± 0.04	n.d.	0.1 ± 0.003	n.d.
NiO	n.d.	0.19 ± 0.05	n.d.	n.d.
CuO	0.47 ± 0.01	0.54 ± 0.07	0.414 ± 0.01	0.39 ± 0.03
SbO <sub>2</sub>	n.d.	n.d.	n.d.	n.d.
ZnO	n.d.	n.d.	n.d.	n.d.
B	0.02 ± 0.0002	n.d.	0.02 ± 0.0002	n.d.
SO <sub>3</sub>	0.58 ± 0.03	n.d.	n.d.	n.d.
Cl	0.76 ± 0.01	1.14 ± 0.8	0.73 ± 0.01	0.87 ± 0.9
Ag	n.d.	n.d.	n.d.	n.d.
Sm	n.d.	n.d.	n.d.	n.d.
Gd	0.0001 ± 0.00001	n.d.	0.00017 ± 0.00001	n.d.
Zr	n.d.	n.d.	n.d.	n.d.
Br	n.d.	n.d.	n.d.	n.d.
Sr	n.d.	n.d.	n.d.	n.d.
Y	n.d.	n.d.	n.d.	n.d.

(continued on next page)



**Fig. 3.** Silica vs. aluminum oxide for the assemblage under study (Palaia Epidavros, Mycenae, Kazarma and Asine) and published Mycenaean parallels (Elateia, Thebes, Rhodes, Tirynths and Kazanaki). The published data are presented with the mean values and their error bars for clarity reasons.

likely these samples were also made with quartz pebbles and the additional alumina could possibly derive from the colorants. In this case the colorant could be the cobaltiferous alums most likely found in Egypt, such as Al-Barnuj oasis deposits in the western desert [24,25].

The high alumina group, comprising samples solely from Mycenae, is quite unique. With the exception of one sample (M1) which has marginal alumina content to the previous group, the rest exhibit very high alumina levels of above 7.00 wt%. Soda glasses with high alumina concentrations are quite rare around the Mediterranean. European Iron Age dark blue glass colored with a cobaltiferous alum that contains up to 8.00 wt% of alumina [26,27] are among the rare examples. Some glass artifacts presenting a wide compositional variability [28,29] have also been noted. Interestingly, in other parts of the world, soda glasses with high alumina concentrations are very common being part of a long tradition. An example of this is found in the Indus region, where the earliest man-made vitrified silica-based material, namely the glaze on steatite beads, dated between 4400 and 3700 BCE, and was compositionally characterized by soda concentrations of approximately 10 wt%, high alumina levels of around 11.00–12.00 wt%, moderate lime concentrations (5.00–6.50 wt%) and low magnesia and potash concentrations, normally < 1.50 wt% [30,32]. High alumina concentrations persist in the subsequent periods and are identified in glasses made in the first millennium BCE becoming a marker of the South Asian glass production [31]. Depending on the type of soda incorporated as a flux, whether obtained from mineral deposits or from plant ashes, two categories are discussed in literature [32].

**5.2.1.2. Alkalies.** The assemblage under study is set against other Mycenaean examples from the literature with respect to their  $K_2O$  vs.  $MgO$  content (Fig. 4) for reasons of comparison and to possibly determine the flux agent used i.e. plant ash or natron. It is clear that all samples are scattered in an area of relatively high magnesium above 2.00 wt%. The chemical composition of plant ashes, among others, typically contains excess of magnesium. It could be, therefore, assumed that the flux agent used in these samples derives from plant ashes.

What is more, the samples seem to form two distinct groups. The HMHK group with potassium oxide levels > 1.00 wt% and the HMLK group with levels of potassium oxide lower than this percentage.

Interestingly, the HMLK group on the lower part of the graph with the low potash content below 1.00 wt% contains samples from all areas apart from Kazarma. These are all cobalt containing samples and this is

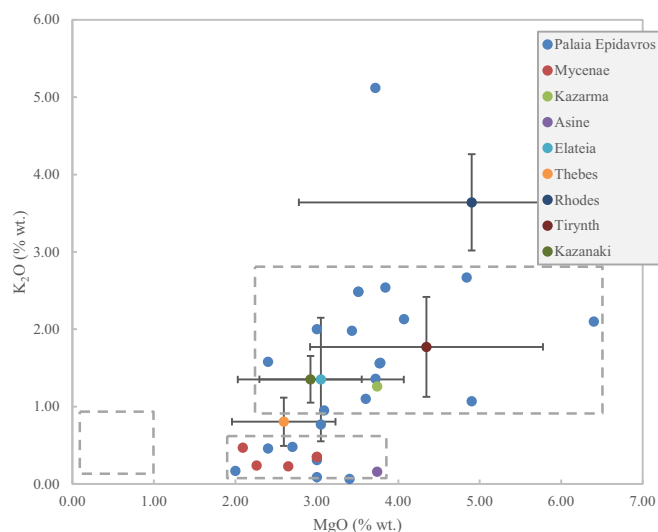


**Fig. 4.** Potassium vs. magnesium oxide for the assemblage under study (Palaia Epidavros, Mycenae, Kazarma and Asine) and published Mycenaean parallels (Elateia, Thebes, Rhodes, Tirynths and Kazanaki). The published data are presented with the mean values and their error bars for clarity reasons.

also the case even for the violet colored ones, which contain some cobalt levels. A speculation that could be made in this respect is the introduction of some cobalt into the batch in order to render the violet hue darker.

This potassium content is characteristic of natron-based glasses, which is normally associated with a magnesium content commonly < 1.00 wt%. Nevertheless, the magnesium levels of these samples are > 2.00 wt%. This is a rather intriguing analytical observation, in which case different explanations could be attempted. First, this excess magnesium could derive from another source either as a deliberate addition or as an impurity. Another approach could move towards this being evidence of another source of natron rich in magnesium or the combined use of natron and plant ashes. This, thus, would suggest the earliest evidence of the use of natron in glassmaking. Furthermore, it is interesting to note that the samples from Mycenae form a rather tight subgroup and this - in association with their high alumina levels - is definitely a rather distinct glass batch.

When the alumina oxide content of the assemblage is plotted against the potassium oxide (Fig. 5) there is a clear pattern seen for the bead samples from Mycenae, all bearing low potassium content and clearly

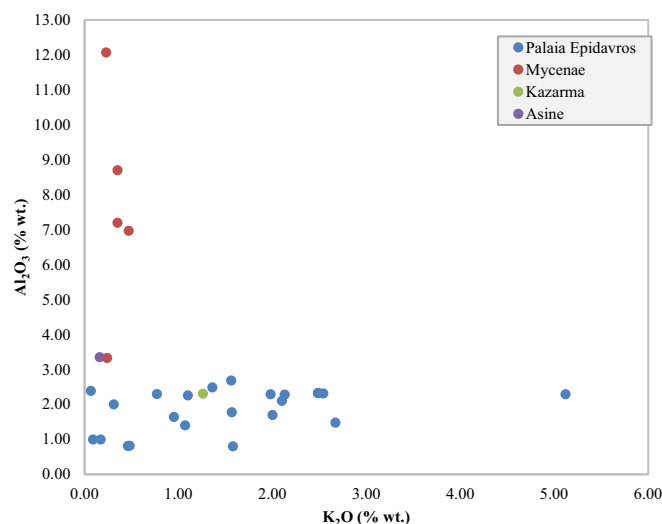


**Fig. 5.** Alumina vs. potassium oxide for the assemblage under study.

deviating from the alumina pattern seen in the rest of the samples. It is interesting to note among the Palaia Epidavros samples that the ones that exhibit alumina levels below 1.70 wt% are all beads, whereas the samples with alumina levels above this and reaching 2.68 wt% are all relief plaques possibly indicating use of raw materials in accordance with typological criteria.

Shortland and Tite [24,25] suggested that a cobalt-bearing alum consisting primarily of pickeringite, a hydrated magnesium aluminum sulfate, was added to a raw glass. The alkali source of Late Bronze glasses is considered to be plant ash, which introduces significant amounts of  $K_2O$  and  $MgO$  to the glass, while soda-rich glass with  $< 1$  wt % of these components is attributed to the use of mineral natron as the alkali source. Therefore, there is a roughly  $2 \pm 3\%$  higher content in  $K_2O$  and  $MgO$  in plant ash glasses, with all other major chemical characteristics, including the aluminum oxide content, being about equal. They, thus, suggest that the raw glass was natron-based, and its level of  $MgO$  has risen to its present level due to the addition of such alum. The HMLK samples from PE fit into this picture. Adding enough of this alum to a natron based glass to introduce the level of cobalt oxide, which normally occurs in cobalt-blue glass, would raise the  $MgO$  levels to levels typically found in plant ash based glasses. The potash level of the glass would not be affected in the absence of  $K_2O$ . The quite constant and elevated level of aluminum oxide could be explained this way, at least qualitatively. All the HMLK samples from P.E., even the ones bearing as a primary colorizer copper, contain cobalt. Three samples from Palaia Epidavros exhibit a deep violet color. All these samples contain minor quantities of cobalt. The introduction of a slight amount of this alum in an attempt to deepen the color of the artifacts could possibly not affect or negligibly affect the alumina levels. Nevertheless, this approach leaves unexplained the similarly elevated levels of alumina in the HMG group.

Following a different train of thought, the low potash content could be explained by the fact that a given plant species can produce a variability of ash compositions affected by regional soil differences, harvesting season, the part of the plant burnt etc. [33–35]. Moreover, different species produce ash of different compositions. Therefore, the raw glass for the cobalt containing blue glass could have been made from ash of a particular plant. This would obviously be different from those plants used for the other glasses. Thus, it could be suggested that the low potash content of the cobalt containing glass might be an indicator of a regional peculiarity of the plant ash used. As pinpointed by Rehren [36], low-potash glasses are not necessarily cobalt-blue glasses. As seen in Lilyquist et al.'s [33] analyses, cobalt-blue glasses tend to exhibit low potash content, but low-potash glasses occur with other primary colorizers as well. Therefore, glasses of any color, as in the studied assemblage, could fit this model. Moreover, this could offer an explanation for the HMG group of samples, whose elevated potassium content could be attributed to a different part of the plant ashed, a different period of harvesting, a totally different plant and so on. A cobaltiferous alum, therefore, could then account for the higher alumina levels.

**5.2.1.3. Colorants.** Regarding the coloration, in the majority of samples both copper and cobalt were detected (Fig. 6). This was somewhat expected since the majority of samples are blue, from dark to light blue, while there are only 4 samples that are violet and one that is turquoise. In two cases that cobalt was not detected (PE 24, PE 26), it was, nevertheless, traced by means of the PGEA analysis (Table 2b). By plotting the samples two major groups are distinguished.

The first grouping entails samples colored with the combination of cobalt and cupric oxide and the second one seems to be purely colored by cupric oxide (based on the XRF analyses), where 3 out of the 5 samples from Mycenae fall. The first occasion has also been noticed in other studies but it is still debated whether a copper containing cobalt mineral was added to the batch to achieve the deep blue, so much favored by the Mycenaean craftsmen, or whether scrap bronze was mixed

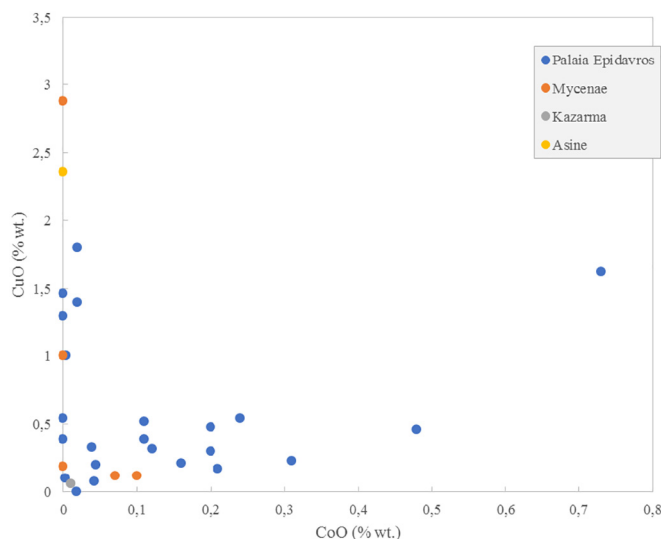
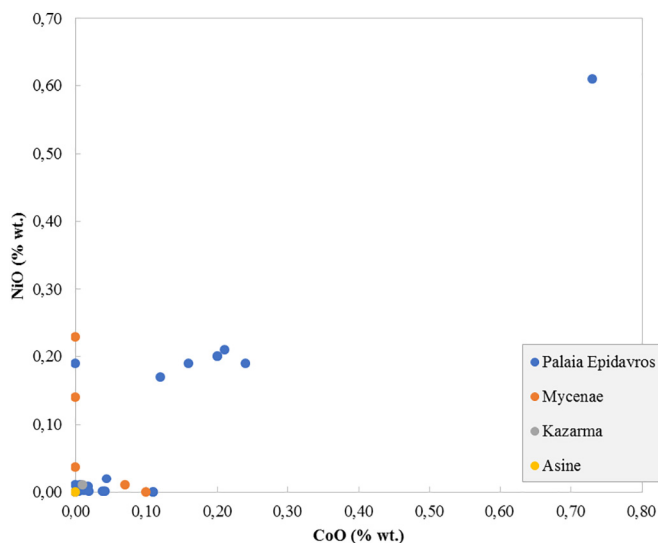


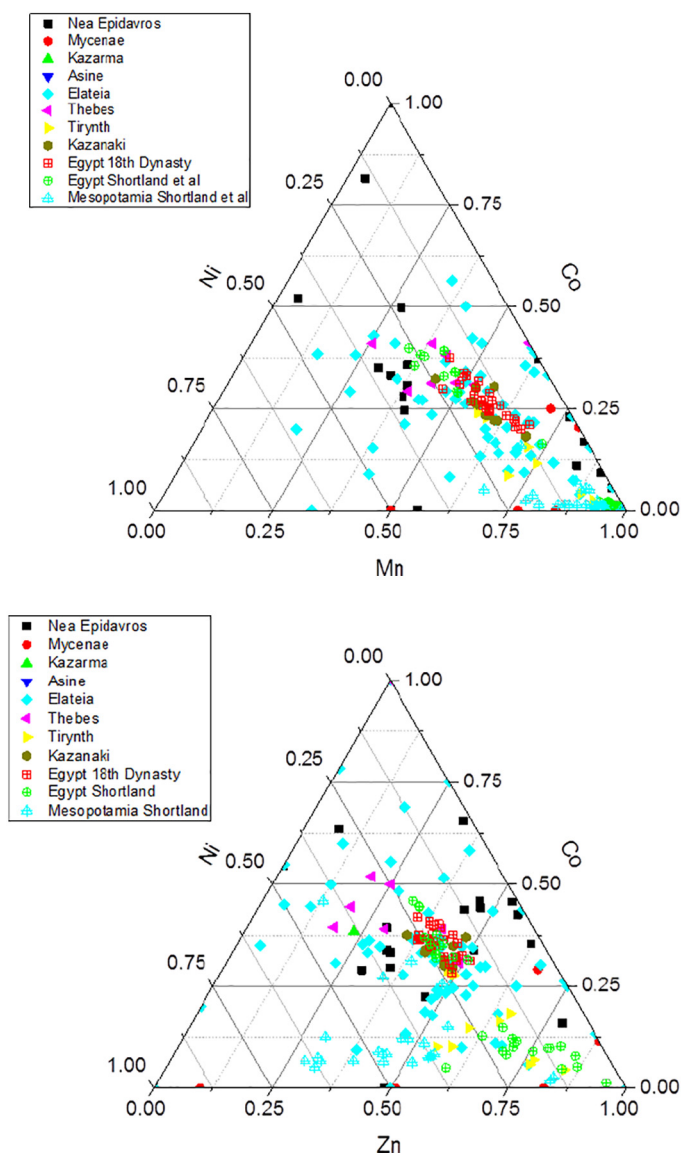
Fig. 6. Copper vs. cobalt oxide for the assemblage under study.

into the cobalt colored batch in order to gain more control of the preferred coloration.

The copper content for the CoCu glasses could be due to its natural occurrence in a cobaltiferous alum. As suggested by Smirniou and Rehren [23] the list of transition metals in the periodic table of Elements associated with such alums of the Western desert runs from manganese through iron, cobalt and nickel to zinc. It is suggested that copper could be part of this series, occurring between nickel and zinc, rendering it possible for copper to be part of the elements that are detected together with cobalt in the Egyptian alum deposits. According to their study, the base glass characteristics for cobalt-blue and CoCu glass are identical within their analytical error range, including levels of alumina and potash, while the other transition metals, manganese, iron, nickel, and zinc, vary compositionally. The variability in the copper should be attributed to the addition of various scrap bronzes and this might account for the existence of tin levels which are not positively correlated in some samples.

A common cobalt source seems to link the vast majority of the samples, while 5 nickel rich samples, which are also arsenic bearing, could be attributed to another cobalt source (Fig. 7). Sample PE15 which has exceptionally high nickel levels (0.61 wt%), exhibits also high cobalt levels (0.73 wt%) and cupric oxide at 1.62 wt% and ferric





Figs. 8–9. Ternary diagrams.

oxide at 1.92 wt% could be a product of recycling.

Ternary diagrams (Figs. 8–9) were attempted to assess the possibility of the correlation of the samples under study with parallels from the literature [37,38]. What can be observed is that, the five samples from Palaia Epidavros, which were pinpointed in the previous figure, cluster together and seem to correspond well with samples from Elateia. Nikita and Henderson [20] suggested for the samples from the latter area the use of a not-established so far copper-containing, arsenic-free though, cobalt mineral to achieve the desired coloration. These samples, nevertheless, contain certain amounts of arsenic. The rest of the samples do not seem to correlate well with the published parallels.

Clearly, at least two different cobalt sources are responsible for the deep blue color in the Palaia Epidavros set of samples. These cobalt sources do not seem to match the one used for the coloration of the samples from Mycenae, where a not clear pattern is seen.

### 5.2.2. PCA

Finally, to further distinguish the samples Principal Component Analysis (PCA) was applied on the major and minor oxides of the

samples excluding colorants and trace elements.

The elemental data obtained from the SEM analyses were normalized at 100%, transformed into base-10 logarithmic values and submitted to a variance-covariance matrix PCA employing algorithms in the STATISTICA 8 Software. From the statistical analysis the first and the third principal components were chosen, which account for almost 73% of the total variance in the dataset.

The PC1-PC3 scores plot illustrated in Fig. 10 reveals a somehow scattered compositional pattern. However, we believe that three distinct groups may be suggested Group A, B and C. The ellipses on this graph were drawn with 95 wt% confidence limit. As it can be seen Group A samples cluster very tight suggesting that they share very common chemical characteristics and therefore the same technology. The majority of Group A samples is the HMK ones with the exception of two. The main characteristic that distinguishes Group A, Group B and Group C samples is the amount of potash as it can be easily seen from the loadings plot (Fig. 11). Furthermore, Group B samples, which are HMLK ones, cluster in the fourth quadrant having excess of calcium. Their average calcium is around 10 wt% which is rather high and in

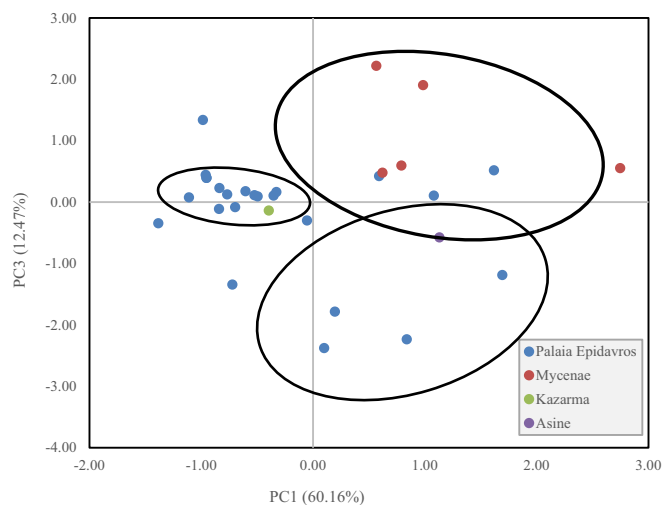


Fig. 10. PCA analysis of all the studied samples.

parallel they have low silica levels with an average of 63 wt%.

An interesting behavior is noted in Group C samples which contains all Mycenaean samples and three samples from Palaia Epidavros. The Mycenaean samples exhibit excess of alumina (average 8.2 wt%), while the Palaia Epidavros samples have moderate alumina levels (average 1.6 wt%). Therefore, we may assume that Group C samples can be distinguished in two subgroups (Group Ci and Group Cii) sharing different manufacturing technologies.

Concluding, through the PCA at least 3 groups of samples are distinguished and the existence of a fourth one is possible. Group A is the most coherent one and most likely these samples share the same technology, group B has interestingly high calcium and low silica content and, finally, in Group C two groups are distinguished, which probably share different technological characteristics.

## 6. Conclusions

It is clear that the samples from the different Argolid sites exhibit different technological characteristics providing new insights into the technology of glass during the Mycenaean period.

The study of specific major and minor elements revealed interesting correlations between samples and pinpointed different glassmaking traditions showing at least one trading route in Eastern Mediterranean,

highlighting Egypt as a possible source of raw glass for glassworkers in the area of Argolid and, more specifically, the area of Palaia Epidavros. Therefore, the majority of samples from Palaia Epidavros show consistent chemical characteristics indicating the same manufacturing center. These samples could be of Egyptian origin and were possibly imported to Greece as glass ingots, rather than readily shaped objects. This is further corroborated by their chemical traits such as their potash content, their silica and soda levels and the chemical fingerprint related to the coloring agent of the cobalt - containing samples, which suggests the use of some cobaltiferous alum possibly from the well - exploited oases in Egypt.

The glassworkers in Palaia Epidavros opt for the wire winding technique for the formation of simple beads and open and molds for the formation of relief plaques with a clear preference for the dark blue color, typically characterizing the vast majority of the assemblages from Mycenaean contexts in general. The possibility, additionally, of firing the artifacts in open fire is not excluded.

The samples from Mycenae form a distinct group presenting a unique technological pattern. Despite sharing common flux characteristics with Egyptian samples, the excess of alumina they exhibit pinpoints towards different technological choices. The excess of alumina can be a marker of a mineral soda or plant ash flux, which would clearly not be commonly used in different workshops of the Mycenaean world and could indicate a complete distinct technology. With the data available so far and the fact that this type of glass has not to the authors' knowledge, been stated so far in literature, it is rather difficult to conclude definitively on the exact type of the alkali source exploited.

Obviously based solely on analytical data and in the absence of glassworking and, most importantly, glassmaking debris and archaeological or textual evidence, sustaining the existence of a primary glass industry would be tentative. Nevertheless, this data provides a basis for assessing this possibility in the light of more evidence in future works.

The application of PCA analysis revealed the existence of two small subgroups having interesting chemical characteristics providing new insights into the technology of the Mycenaean glass.

Finally, within the framework of a large research program - part of which is this study - further investigation of assemblages from other key-sites in Peloponnese is carried out. The present data alongside with data from ongoing analyses of the parallel assemblages aspires to contribute to our understanding of the glassworking and/or glass-making industry in the Mycenaean world and enlighten a significant aspect of the material culture in Aegean.

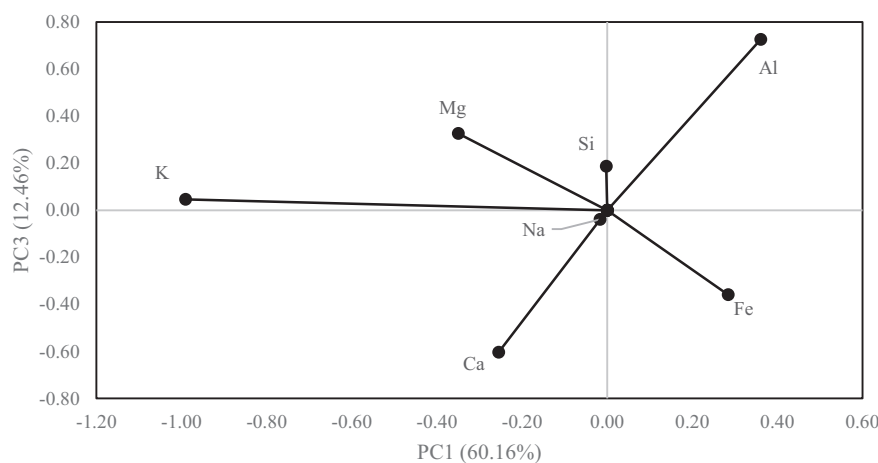


Fig. 11. PCA analysis of all the studied samples with respect to their major elements content.



**Acknowledgements**

The authors acknowledge a grant (N.Z. as the proposal leader and beneficiary and M.K. as a beneficiary), provided by the CHARISMA SEVENTH FRAMEWORK PROGRAMME Research infrastructures

INFRA-2008-1.1.1 Bottom-up approach (Grant Agreement No. 228330), covering transportation and accommodation at FIXLAB facilities at the Budapest Neutron Centre, for the performance of PGAA measurements.

**Appendix A**

Table 1  
Chronology of the Late Bronze Age [4].

Date (BCE)	Crete	Cyclades	Mainland Greece	Egypt
3100	Early Minoan I	Early Cycladic I	Early Helladic I	1st–2nd Dynasty (3100/3000–2700)
3000				
2900	Early Minoan IIA	Early Cycladic II	Early Helladic IIA	<b>Old Kingdom</b> (2700–2136)
2800				
2700	Early Minoan IIB	Early Helladic IIB		
2600	Early Minoan III	Early Cycladic III	Early Helladic III	1st Intermediate Period (2136–2023)
2500				
2400	Middle Minoan IA	Middle Cycladic I	Middle Helladic I	<b>Middle Kingdom</b> (2116–1795)
2300				
2200	Middle Minoan IB	Middle Cycladic II	Middle Helladic II	
2100	Middle Minoan II			
2000	Middle Minoan III	Middle Cycladic III	Middle Helladic III	2nd Intermediate Period (1795–1540)
1900				
1800	Late Minoan IA	Late Cycladic I	Late Helladic I	<b>New Kingdom</b>
1700				
1600	Late Minoan IB	Late Cycladic II	Late Helladic IIA	
1500	Late Minoan II		Late Helladic IIB	
1400	III A1	Late Cycladic III	Late Helladic III A1	-19th Dynasty (1295–1186)
1300	III A2		Late Helladic III A2	Ramses II 1279–1213
1200	Late Minoan IIIB		Late Helladic IIIB	-20th Dynasty (1186–1070)
1100	Late Minoan IIIC	Late Helladic IIIC	Ramses III (1184–1153)	
1000	Subminoan Submycenaean			

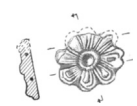
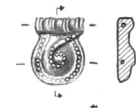
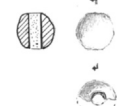
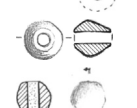


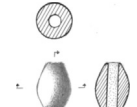
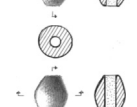





Table 2

Sampled areas.

Area	Excavator	Tombs	Number of samples	Dating
Palaia Epidavros (Plots: D. Koutselopoulos, Venizelos)	V. Stais A. Piteros	Tombs 1–2–3–4 Tomb 2-B Stai	35	Tomb 1: LBIIIB Tombs 2–3: LBII–LBIIIA Tomb 4: LBIIIA–LBIIIB1 Tomb 2-B Stai: LBIIIA–LBIIIB
Mycenae Tomb 3-drains 7e and 8e	El. Palaiologou		8	LBIIIA–LBIIIB
Ancient Asine (Plot: Sp. Gogonas)	A. Piteros	Tomb 1	5	LBII–LBIIIC
Kazarma	Protonotariou-Deilaki	Tholos tomb	1	LBII–LBIIIC

Table 3

Description of the samples. PE stands for Palaia Epidavros, M for Mycenae, AA for ancient Asine and K for Kazarma.

n.	Sample	Colour	Dating (BCE)	Object (bead or plaque)	Archaeological drawings
1.	PE1	Transparent deep blue	1330–1060	Plaque-double rosette	
2.	PE2	Transparent deep blue	1330–1060	Plaque-simple volute (type A)	
3.	PE4	Opaque violet	1330–1190	Bead fragment-simple spherical	
4.	PE5	Opaque violet	1330–1190	Bead-barrel shaped	
5.	PE6	Opaque violet	1330–1190	Bead fragment-simple spherical	
6.	PE7	Transparent deep blue	1600–1330	Bead fragment-simple spherical	
7.	PE8	Transparent deep blue	1600–1330	Bead fragment-simple round	
8.	PE10	Transparent deep blue	1600–1330	Bead fragment-simple round	
9.	PE11	Opaque light blue	1600–1330	Bead-barrel shaped	
10.	PE13	Opaque light blue	1600–1330	Bead-barrel shaped	
11.	PE15	Transparent deep blue	1600–1330	Bead-cylindrical with bands	
12.	PE21	Transparent deep blue	1600–1330	Plaque-single volute hanging from bar	
13.	PE22	Transparent deep blue	1600–1330	Plaque-single volute hanging from bar	
14.	P23	Transparent deep blue	1600–1330	Plaque-ivy leaf	
15.	PE24	Transparent deep blue	1600–1330	Plaque-ivy leaf	

16.	PE25	Transparent deep blue	1600–1330	Plaque-ivy leaf
17.	PE26	Transparent deep blue	1600–1330	Plaque-ivy leaf
18.	PE28	Opaque light blue	1600–1330	Bead-simple spherical
19.	PE29	Transparent deep blue	1600–1330	Bead-simple spherical
20.	PE30	?	1600–1330	Plaque-cockleshell
21.	PE32	Transparent deep blue	1600–1330	Plaque-suspended curl on plaque hanging from a bar
22.	PE33	Transparent deep blue	1600–1330	Plaque-suspended curl on plaque hanging from a bar
23.	PE34	Transparent deep blue	1600–1330	Plaque-suspended curl on plaque hanging from a bar
24.	M1	Opaque turquoise	1600–1060	Bead-simple spherical
25.	M3	Transparent deep blue?	1600–1060	Bead-barrel shaped with incised bands
26.	M5	Transparent deep blue?	1600–1060	Plait plaque hanging from a bar or rosette
27.	M7	Opaque light blue?	1600–1060	Bead-simple spherical
28.	M8	Transparent deep blue?	1600–1060	Plaque-volute hanging from a bar
29.	AA5	Opaque light blue	1600–1060	Bead-discoïd crenellated
30.	K1	Translucent light purple	1600–1060	Bead-spherical bead perimetrically engrooved

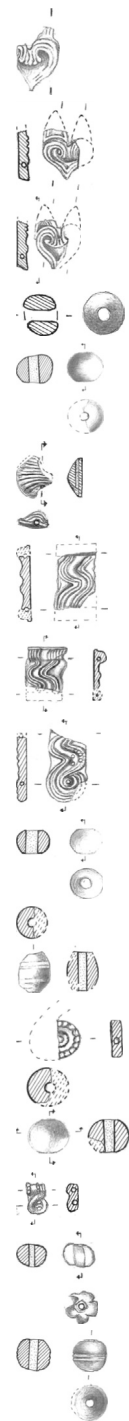


Table 4  
Results obtained by means of SEM/EDS and XRF (n.d.: not detected).

		PE1	P2	PE4	PE5	PE6	PE7	PE8	PE10
SEM/EDX analysis	SiO <sub>2</sub>	65.31 ± 1.91	64.49 ± 1.93	64.01 ± 1.84	60.02 ± 1.86	72.01 ± 2.01	62.01 ± 1.79	65.02 ± 1.85	59.01 ± 1.76
	Na <sub>2</sub> O	16.95 ± 1.51	15.71 ± 1.32	22.02 ± 1.99	13.01 ± 1.11	12.01 ± 0.98	23.51 ± 1.75	14.6 ± 1.02	22.01 ± 1.78
	CaO	6.98 ± 0.66	6.27 ± 0.61	5.81 ± 0.61	19.09 ± 1.79	7.21 ± 0.62	5.01 ± 0.44	11.3 ± 1.01	4.91 ± 0.39
	MgO	3.01 ± 0.29	4.07 ± 0.36	2.71 ± 0.29	2.41 ± 0.22	2.40 ± 0.25	3.61 ± 0.32	3.40 ± 0.29	6.39 ± 0.54
	K <sub>2</sub> O	2.02 ± 0.19	2.13 ± 0.21	0.48 ± 0.03	0.46 ± 0.05	1.58 ± 0.13	1.09 ± 0.12	0.07 ± 0.01	2.11 ± 0.19
	Al <sub>2</sub> O <sub>3</sub>	1.71 ± 0.15	2.28 ± 0.23	0.82 ± 0.09	0.81 ± 0.10	0.81 ± 0.10	2.26 ± 0.21	2.39 ± 0.22	2.12 ± 0.21
XRF analysis	P <sub>2</sub> O <sub>5</sub>	0.19 ± 0.01	0.21 ± 0.01	n.d.	0.99 ± 0.09	0.12 ± 0.01	0.12 ± 0.01	0.001	0.03 ± 0.001
	SO <sub>4</sub>	0.62 ± 0.05	0.60 ± 0.05	0.48 ± 0.03	0.11 ± 0.01	0.51 ± 0.04	0.81 ± 0.07	0.07 ± 0.001	1.20 ± 0.11
	Cl <sub>2</sub> O	1.11 ± 0.09	0.87 ± 0.07	n.d.	n.d.	0.29 ± 0.02	0.08 ± 0.001	n.d.	0.02 ± 0.001
	TiO <sub>2</sub>	n.d.	0.21 ± 0.02	0.91 ± 0.07	0.70 ± 0.07	0.14 ± 0.01	n.d.	0.10 ± 0.01	n.d.
	MnO	0.19 ± 0.02	n.d.	0.69 ± 0.05	0.57 ± 0.05	0.84 ± 0.07	0.02 ± 0.001	0.63 ± 0.05	0.04 ± 0.003
	Fe <sub>2</sub> O <sub>3</sub>	0.71 ± 0.06	0.89 ± 0.07	0.81 ± 0.08	1.21 ± 0.11	0.98 ± 0.07	1.00 ± 0.09	1.69 ± 0.14	0.22 ± 0.02
	CoO	0.21 ± 0.03	0.11 ± 0.02	0.01 ± 0.002	0.01 ± 0.002	0.003	0.04 ± 0.01	0.04 ± 0.008	0.0044
	CuO	0.29 ± 0.02	0.39 ± 0.02	0.001	0.01 ± 0.001	0.09 ± 0.001	0.18 ± 0.01	0.33 ± 0.06	1.00 ± 0.09
	Ba	n.d.	n.d.	n.d.	n.d.	n.d.	n.d.	0.01	n.d.
	V	n.d.	n.d.	n.d.	n.d.	n.d.	n.d.	n.d.	n.d.
	Cr <sub>2</sub> O <sub>3</sub>	n.d.	0.21 ± 0.04	0.80 ± 0.13	0.007	0.01 ± 0.002	0.12 ± 0.01	0.31 ± 0.05	0.99 ± 0.16
	NiO	0.2	n.d.	0.01	0.001	0.001	0.02 ± 0.002	0.001	0.0003
	ZnO	0.2	n.d.	0.007	0.005	0.015	0.01 ± 0.002	0.02 ± 0.003	0.008
	As <sub>2</sub> O <sub>3</sub>	n.d.	0.99 ± 0.17	0.001	0.003	n.d.	0.01 ± 0.002	n.d.	0.001
	PbO	0.001	n.d.	0.04 ± 0.008	0.57 ± 0.11	n.d.	0.01 ± 0.002	0.01 ± 0.002	n.d.
	Br	n.d.	n.d.	n.d.	n.d.	n.d.	n.d.	n.d.	n.d.
	Sr	0.009	n.d.	n.d.	n.d.	n.d.	n.d.	n.d.	n.d.
	Y	n.d.	n.d.	n.d.	n.d.	n.d.	n.d.	n.d.	n.d.
	Zr	0.004	n.d.	n.d.	n.d.	n.d.	n.d.	n.d.	n.d.
	SnO <sub>2</sub>	n.d.	n.d.	0.69 ± 0.11	0.57 ± 0.11	n.d.	0.02 ± 0.004	0.03 ± 0.005	n.d.
Sb <sub>2</sub> O <sub>5</sub>	n.d.	n.d.	0.06 ± 0.01	0.007	n.d.	0.04 ± 0.007	0.006	0.06 ± 0.01	
Sum		99.7	98.5	100.3	100.6	99.0	99.9	100.0	100.1

		PE11	PE13	PE15	PE21	PE22	P24	PE23
SEM/EDX analysis	SiO <sub>2</sub>	62.11 ± 1.84	66.35 ± 1.99	60.89 ± 1.86	64.75 ± 1.89	64.33 ± 1.71	64.96 ± 1.96	64.99 ± 1.85
	Na <sub>2</sub> O	19.01 ± 1.56	14.39 ± 1.32	12.78 ± 1.32	18.29 ± 1.72	17.32 ± ± 1.65	15.92 ± 1.42	15.41 ± 0.01
	CaO	5.31 ± 0.53	6.85 ± 0.62	8.21 ± 0.79	6.03 ± 0.56	8.31 ± 0.73	6.19 ± 0.55	5.99 ± 0.56
	MgO	4.89 ± 0.54	4.84 ± 0.41	3.72 ± 0.34	3.84 ± 0.31	3.78 ± 0.38	3.51 ± 0.34	3.42 ± 0.33
	K <sub>2</sub> O	1.07 ± 0.09	2.67 ± 0.24	5.12 ± 0.43	2.54 ± 0.23	1.57 ± 0.16	2.49 ± 0.22	2.56 ± 0.23
	Al <sub>2</sub> O <sub>3</sub>	1.40 ± 0.13	1.48 ± 0.12	2.29 ± 0.21	2.31 ± 0.19	1.78 ± 0.18	2.33 ± 0.19	2.42 ± 0.23
XRF analysis	P <sub>2</sub> O <sub>5</sub>	0.01 ± 0.001	0.62 ± 0.05	0.13 ± 0.01	0.11 ± 0.01	0.09 ± 0.001	0.23 ± 0.01	0.21 ± 0.02
	SO <sub>4</sub>	1.07 ± 0.10	0.55 ± 0.04	n.d.	0.66 ± 0.05	0.40 ± 0.005	0.62 ± 0.05	0.49 ± 0.05
	Cl <sub>2</sub> O	0.44 ± 0.03	0.62 ± 0.06	1.29 ± 0.11	0.12 ± 0.01	0.24 ± 0.02	1.14 ± 0.12	1.12 ± 0.11
	TiO <sub>2</sub>	0.51 ± 0.01	0.08 ± 0.001	0.5 ± 0.04	0.11 ± 0.01	n.d.	0.31 ± 0.01	0.11 ± 0.01
	MnO	0.99 ± 0.08	0.01 ± 0.0001	0.06 ± 0.001	0.17 ± 0.01	0.26 ± 0.02	0.24 ± 0.02	0.22 ± 0.02
	Fe <sub>2</sub> O <sub>3</sub>	0.49 ± 0.03	0.53 ± 0.04	1.92 ± 1.81	0.71 ± 0.05	0.61 ± 0.06	0.73 ± 0.06	0.69 ± 0.05
	CoO	0.02 ± 0.001	n.d.	0.73 ± 0.11	0.21 ± 0.04	0.21 ± 0.03	0.24 ± 0.04	n.d.
	CuO	1.81 ± 0.16	1.46 ± 0.12	1.62 ± 0.15	0.48 ± 0.04	0.17 ± 0.01	0.54 ± 0.05	0.51 ± 0.04
	Ba	n.d.	n.d.	n.d.	n.d.	n.d.	n.d.	n.d.
	V	n.d.	n.d.	n.d.	n.d.	n.d.	n.d.	n.d.
	Cr <sub>2</sub> O <sub>3</sub>	1.03 ± 0.11	0.11 ± 0.01	n.d.	n.d.	n.d.	n.d.	0.04 ± 0.008
	NiO	0.001	0.01 ± 0.002	0.61 ± 0.11	0.21 ± 0.04	0.21 ± 0.04	0.19 ± 0.04	0.17 ± 0.04
	ZnO	0.03 ± 0.006	n.d.	n.d.	0.19 ± 0.003	0.20 ± 0.01	0.18 ± 0.04	0.19 ± 0.03
	As <sub>2</sub> O <sub>3</sub>	0.002	n.d.	n.d.	0.003	0.003	n.d.	n.d.
	PbO	n.d.	n.d.	n.d.	0.05 ± 0.01	0.004	n.d.	n.d.
	Br	n.d.	n.d.	n.d.	0.001	n.d.	n.d.	n.d.
	Sr	n.d.	n.d.	n.d.	n.d.	0.05	n.d.	n.d.
	Y	n.d.	n.d.	n.d.	0.001	n.d.	n.d.	n.d.
	Zr	n.d.	n.d.	n.d.	n.d.	0.005	n.d.	n.d.
	SnO <sub>2</sub>	n.d.	n.d.	n.d.	n.d.	0.001	n.d.	n.d.
Sb <sub>2</sub> O <sub>5</sub>	n.d.	n.d.	n.d.	n.d.	0.12 ± 0.02	n.d.	n.d.	
Sum		99.3	100.6	99.9	100.7	99.7	99.8	99.4

(continued on next page)



Table 4 (continued)

		PE25	PE26	PE28	PE29	PE30	PE32	PE33	PE34	
SEM/EDX analysis	SiO <sub>2</sub>	65.02 ± 1.91	63.54 ± 1.80	65.19 ± 1.92	66.99 ± 2.11	63.03 ± 1.89	64.21 ± 1.94	63.88 ± 1.79	65.01 ± 1.95	
	Na <sub>2</sub> O	15.91 ± 1.42	18.85 ± 1.61	19.72 ± 1.43	19.98 ± 1.91	19.04 ± 1.79	16.61 ± 1.49	17.02 ± 1.63	22.99 ± 1.62	
	CaO	4.70 ± 0.61	6.74 ± 0.99	5.68 ± 0.79	5.61 ± 0.79	13.01 ± 0.97	8.42 ± 0.85	8.16 ± 0.64	2.10 ± 0.31	
	MgO	3.05 ± 0.31	3.43 ± 0.36	3.09 ± 0.29	3.02 ± 0.31	2.01 ± 0.26	3.77 ± 0.41	3.72 ± 0.35	3.00 ± 0.29	
	K <sub>2</sub> O	0.77 ± 0.05	1.98 ± 0.12	0.95 ± 0.08	0.09 ± 0.006	0.17 ± 0.01	1.56 ± 0.11	1.36 ± 0.09	0.31 ± 0.006	
	Al <sub>2</sub> O <sub>3</sub>	2.31 ± 0.21	2.29 ± 0.21	1.64 ± 0.15	1.00 ± 0.11	1.01 ± 0.11	2.68 ± 0.24	2.49 ± 0.27	2.00 ± 0.18	
XRF analysis	P <sub>2</sub> O <sub>5</sub>	n.d.	0.21 ± 0.03	0.002 ± 0.0003	n.d.	n.d.	0.10 ± 0.02	0.12 ± 0.02	n.d.	
	SO <sub>4</sub>	0.77 ± 0.08	n.d.	0.12 ± 0.01	0.09 ± 0.0001	0.17 ± 0.01	0.53 ± 0.11	n.d.	0.17 ± 0.06	
	Cl <sub>2</sub> O	0.003 ± 0.0001	0.87 ± 0.07	n.d.	0.001 ± 0.0002	n.d.	0.04 ± 0.001	0.78 ± 0.15	n.d.	
	TiO <sub>2</sub>	0.002 ± 0.0001	n.d.	0.62 ± 0.03	0.12 ± 0.01	1.61 ± 0.31	0.69 ± 0.14	0.33 ± 0.06	0.99 ± 0.08	
	MnO	0.14 ± 0.03	n.d.	0.22 ± 0.01	0.61 ± 0.11	0.001	0.19 ± 0.01	0.20 ± 0.03	0.14 ± 0.03	
	Fe <sub>2</sub> O <sub>3</sub>	1.41 ± 0.13	0.91 ± 0.08	0.52 ± 0.04	0.12 ± 0.02	0.48 ± 0.03	0.85 ± 0.07	0.82 ± 0.07	0.99 ± 0.09	
	CoO	0.02 ± 0.004	n.d.	0.16 ± 0.003	0.007 ± 0.001	0.013 ± 0.002	0.11 ± 0.01	0.12 ± 0.02	0.04 ± 0.008	
	CuO	1.41 ± 0.12	0.39 ± 0.03	0.21 ± 0.02	1.30 ± 0.11	0.006 ± 0.0001	0.52 ± 0.11	0.32 ± 0.11	0.07 ± 0.01	
	Ba	n.d.	n.d.	n.d.	n.d.	0.0193 ± 0.004	n.d.	n.d.	n.d.	
	V	n.d.	n.d.	n.d.	n.d.	n.d.	n.d.	n.d.	n.d.	
	Cr <sub>2</sub> O <sub>3</sub>	1.21 ± 0.22	n.d.	n.d.	1.10	0.001 ± 0.0001	0.01 ± 0.001	0.01 ± 0.002	n.d.	
	NiO	0.01 ± 0.002	n.d.	0.19	0.002	0.002 ± 0.0004	n.d.	0.17 ± 0.03	0.001	
	ZnO	0.03 ± 0.006	n.d.	0.19	0.007	0.01 ± 0.0003	n.d.	0.25 ± 0.06	0.05 ± 0.01	
	As <sub>2</sub> O <sub>3</sub>	n.d.	0.002	0.1	n.d.	n.d.	0.01 ± 0.001	0.001	0.002	
	PbO	n.d.	n.d.	n.d.	0.01 ± 0.0002	0.01 ± 0.0001	0.006	0.003	0.01 ± 0.002	
	Br	n.d.	n.d.	n.d.	n.d.	n.d.	n.d.	n.d.	n.d.	
	Sr	n.d.	n.d.	n.d.	n.d.	n.d.	0.06 ± 0.01	0.054 ± 0.001	n.d.	
	Y	n.d.	n.d.	n.d.	n.d.	n.d.	n.d.	0.001	n.d.	
	Zr	n.d.	n.d.	n.d.	n.d.	n.d.	0.005	0.007	n.d.	
	SnO <sub>2</sub>	0.14 ± 0.01	n.d.	0.002 ± 0.0001	0.60 ± 0.11	0.001	n.d.	n.d.	0.14 ± 0.03	
	Sb <sub>2</sub> O <sub>5</sub>	n.d.	n.d.	n.d.	n.d.	0.01 ± 0.01	n.d.	n.d.	0.06 ± 0.01	
	Sum		96.94	99.2	98.8	100.6	100.6	100.4	99.8	98.1
			M1	M3	M5	M7	M8	K1	AA5	
SEM/EDX analysis	SiO <sub>2</sub>	69.93 ± 2.1	65.1 ± 1.93	63.45 ± 1.80	67.01 ± 2.01	68.1 ± 2.41	67.71 ± 1.99	66.68 ± 2.11		
	Na <sub>2</sub> O	11.59 ± 1.39	11.65 ± 1.48	7.8 ± 0.99	12.72 ± 1.45	12.62 ± 1.60	11.92 ± 1.22	12.26 ± 1.09		
	CaO	4.28 ± 0.43	4.83 ± 0.79	8.84 ± 0.69	6.2 ± 0.98	5.01 ± 0.97	7.59 ± 1.11	7.46 ± 0.87		
	MgO	2.26 ± 0.28	2.65 ± 0.21	2.09 ± 0.29	3.00 ± 0.29	3.02 ± 0.28	3.74 ± 0.31	3.74 ± 0.32		
	K <sub>2</sub> O	0.24 ± 0.005	0.23 ± 0.005	0.47 ± 0.04	0.35 ± 0.006	0.35 ± 0.006	1.26 ± 0.09	0.16 ± 0.006		
	Al <sub>2</sub> O <sub>3</sub>	3.33 ± 0.25	12.07 ± 1.22	6.97 ± 0.57	7.21 ± 0.59	8.71 ± 0.71	2.31 ± 0.19	3.35 ± 0.27		
	P <sub>2</sub> O <sub>5</sub>	n.d.	0.17 ± 0.01	0.22 ± 0.01	n.d.	0.11 ± 0.01	0.32 ± 0.06	n.d.		
	XRF analysis	SO <sub>4</sub>	0.29 ± 0.06	n.d.	0.87 ± 0.17	0.04 ± 0.01	n.d.	0.09 ± 0.02	0.19 ± 0.01	
		Cl <sub>2</sub> O	0.34 ± 0.05	0.21 ± 0.05	0.83 ± 0.16	0.06	0.12 ± 0.02	0.88 ± 0.15	0.08 ± 0.02	
		TiO <sub>2</sub>	0.31 ± 0.02	0.28 ± 0.02	0.21 ± 0.02	0.17 ± 0.02	0.21 ± 0.02	0.08 ± 0.01	0.23 ± 0.02	
		MnO	0.47 ± 0.03	0.20 ± 0.03	1.30 ± 0.21	0.04 ± 0.001	0.39 ± 0.07	1.02 ± 0.19	0.07 ± 0.01	
Fe <sub>2</sub> O <sub>3</sub>		1.06 ± 0.11	1.01 ± 0.20	1.32 ± 0.24	1.99 ± 0.17	0.38 ± 0.08	1.12 ± 0.09	2.41 ± 0.21		
CoO		n.d.	0.07 ± 0.001	n.d.	n.d.	0.11 ± 0.01	0.01 ± 0.002	n.d.		
CuO		1.00 ± 0.11	0.12 ± 0.01	2.88 ± 0.15	0.19 ± 0.01	0.12 ± 0.01	0.06 ± 0.001	2.16 ± 0.16		
Ba		n.d.	n.d.	n.d.	n.d.	n.d.	n.d.	n.d.		
V		n.d.	n.d.	n.d.	n.d.	n.d.	n.d.	n.d.		
Cr <sub>2</sub> O <sub>3</sub>		n.d.	n.d.	0.71 ± 0.12	n.d.	0.14 ± 0.03	n.d.	0.06 ± 0.01		
NiO		0.14 ± 0.03	0.01 ± 0.002	0.23 ± 0.05	0.04 ± 0.001	n.d.	0.01 ± 0.001	n.d.		
ZnO		0.66 ± 0.12	0.16 ± 0.22	0.24 ± 0.05	0.004	0.76 ± 0.12	0.006	n.d.		
As <sub>2</sub> O <sub>3</sub>		n.d.	n.d.	n.d.	n.d.	0.16	n.d.	n.d.		
PbO	n.d.	n.d.	n.d.	n.d.	n.d.	n.d.	n.d.			
Br	n.d.	n.d.	n.d.	n.d.	n.d.	n.d.	n.d.			
Sr	n.d.	n.d.	n.d.	n.d.	n.d.	n.d.	n.d.			
Y	n.d.	n.d.	n.d.	n.d.	n.d.	n.d.	n.d.			
Zr	n.d.	n.d.	n.d.	n.d.	n.d.	n.d.	n.d.			
SnO <sub>2</sub>	n.d.	n.d.	n.d.	n.d.	n.d.	n.d.	n.d.			
Sb <sub>2</sub> O <sub>5</sub>	2.54 ± 0.51	n.d.	n.d.	n.d.	n.d.	n.d.	1.52			
Sum		98.4	98.8	98.4	99.0	100.3	98.1	100.4		

## References

- [1] J. Henderson, *Ancient Glass, an Interdisciplinary Exploration*, Cambridge University Press, New York and Cambridge, 2013.
- [2] N. Zacharias, M. Kaparou, Sz. Kasztovszky, B. Maroti, K. Beltsios, J. Murphy, V. Kantarelou, A.G. Karydas, An alteration and provenance study of Mycenaean glass objects using neutron beam and X-ray methods, *Archeometriai Muhely 2013/ X./2* (2013) 127–140.
- [3] K. Shelton, Mainland Greece, in: E.H. Cline (Ed.), *The Oxford Handbook of the Bronze Age Aegean*, Oxford University Press, Oxford, 2010, pp. 139–148.
- [4] C.W. Shelmerdine, Background, sources and methods, in: C.W. Shelmerdine (Ed.), *The Cambridge Companion to the Aegean Bronze Age*, Cambridge University Press, 2008, pp. 1–18 σελ.
- [5] *Archaeological Deltion* 44, (1989), pp. 129–131 (in Greek).
- [6] *Archaeological Deltion* 50, B1 Chronika, (1995) (in Greek).
- [7] *Archaeological Deltion* 24, (1969), pp. 104–105 (in Greek).
- [8] J. Goldstein, D.E. Newbury, D.C. Joy, C.E. Lyman, P. Echlin, E. Lifshin, L. Sawyer, J.R. Michael, *Scanning Electron Microscopy and X-ray Microanalysis*, 3rd edition, Springer, 2003.
- [9] A. Oikonomou, K. Beltsios, N. Zacharias, Analytical and technological study of blue glass from Thebes, Greece: an overall assessment, in: D. Ignatiadou, A. Antonaras (Eds.), *Proceedings of the AIHV 18, 2012*, pp. 75–80. Thessaloniki.
- [10] N. Zacharias, L. Beltsios, A. Oikonomou, A.G. Karydas, Y. Bassiakos, C.T. Michael, Ch. Zarkadas, Solid-state luminescence for the optical examination of archaeological glass beads, *Opt. Mater.* 30 (7) (2008) 1127–1133.
- [11] D. Sokaras, A.G. Karydas, A. Oikonomou, N. Zacharias, K. Beltsios, V. Kantarelou, Combined elemental analysis of ancient glass beads by means of ion beam, portable XRF, and EPMA techniques, *Anal. Bioanal. Chem.* 395 (7) (2009) 2199–2209.
- [12] A. Moropoulou, N. Zacharias, E.T. Delegou, B. Maróti, Zs. Kasztovszky, Analytical and technological examination of glass tesserae from Hagia Sophia, *Microchem. J.* 126 (2016) 170–184.
- [13] Zs. Révay, T. Belgya, Principles of PGAA method, in: G.L. Molnár (Ed.), *Handbook of Prompt Gamma Activation Analysis with Neutron Beams*, Kluwer Academic Publishers, Dordrecht/Boston/New York, 2004, pp. 1–30.
- [14] L. Szentmiklósi, Zs. Révay, T. Belgya, A. Simonits, Z. Kis, Combining prompt gamma activation analysis with off-line counting, *J. Radioanal. Nucl. Chem.* 278 (2008) 657–660.
- [15] Zs. Révay, T. Belgya, L. Szentmiklósi, G.L. Molnár, Prompt gamma activation analysis using a chopped neutron beam, *J. Radioanal. Nucl. Chem.* 264 (2005) 277–281.
- [16] Zs. Révay, Determining elemental composition using prompt g activation analysis, *Anal. Chem.* 81 (2009) 6851–6859.
- [17] L. Szentmiklósi, K. Gméling, Z. Révay, Fitting the boron peak and resolving interferences in the 450–490 keV region of PGAA spectra, *J. Radioanal. Nucl. Chem.* 271 (2007) 447–453.
- [18] Zs. Kasztovszky, K.T. Biró, A. Markó, V. Dobosi, Cold neutron prompt gamma activation analysis—a non-destructive method for characterization of high silica content chipped stone tools and raw materials, *Archaeometry* 50 (1) (2008) 12–29.
- [19] Zs. Kasztovszky, J. Kunicki-Goldfinger, Applicability of Prompt Gamma Activation Analysis to glass archaeometry, in: I. Turbanti-Memmi (Ed.), *Proceedings of the 37th International Symposium on Archaeometry*, Springer-Verlag, Berlin Heidelberg, 2011, pp. 83–90.
- [20] N. Zacharias, E. Palamara, Fuxi Gan, Qinghui Li, Julian Henderson (Eds.), Chapter 12: Glass Corrosion: Issues and Approaches for Archaeological Science in Recent Advances in the Scientific Research on Ancient Glass and Glasses, *World Scientific*, 2016, pp. 233–248; K. Nikita, J. Henderson, Glass analyses from Mycenaean Thebes and Elateia: compositional evidence for a Mycenaean glass industry, *J. Glass Stud.* 48 (2006) 71–120.
- [21] L. Hench, D.E. Clark, Physical chemistry of glass surfaces, *J. Non-Cryst. Solids* 48 (1978) 83–105; P. Triantafyllidis, I. Karatasios, Late bronze age glass production on Rhodes, Greece, *J. Glass Stud.* 54 (2012) 25–32.
- [22] A. Shortland, M. Tite, Raw materials of glass from Amarna and implications for the origins of Egyptian glass, *Archaeometry* 42 (2000) 141–151; M.S. Walton, A.J. Shortland, S. Kirk, P. Degryse, Evidence for the trade of Mesopotamian and Egyptian glass to Mycenaean Greece, *J. Archaeol. Sci.* 36 (2009) 1496–1503.
- [23] M. Smirniou, Th. Rehren, V. Adrymi-Sismani, E. Asderaki, B. Gratuze, Mycenaean beads from Kazanaki, Volos: a further node in LBA glass network, *AIHV Ann. 18e Congrès* (2012) 11–18.
- [24] A. Shortland, M.S. Tite, Raw materials of glass from Amarna and implications for the origins of Egyptian glass, *Archaeometry* 42 (2000) 141–151.
- [25] A. Shortland, L. Schachner, I. Freestone, M. Tite, Natron as a flux in the early vitreous materials industry: sources, beginnings and reasons for decline, *J. Archaeol. Sci.* 33 (2006) 521–530.
- [26] B. Gratuze, Les premiers verres au natron retrouvés en Europe occidentale: composition chimique et chrono-typologie, *AIHV Ann. 18e Congrès* (2009) 8–14.
- [27] B. Gratuze, M. Picon, Utilisation par l'industrie verrière des sels d'aluns des oasis égyptiennes au début du premier millénaire avant notre ère, in: P. Borgard, J.P. Brun, M. Picon (Eds.), *L'alun de Méditerranée*, Collection du Centre Jean Bérard 23, Naples, 2005, pp. 269–276.
- [28] L. Montanaro, J.M. Tulliani, P. Palmero, A. Negro, Chemical composition of some Roman glass tesserae discovered in a calidarium located in Northern Italy, *Silic. Ind.* 68 (11–12) (2003) 151–155.
- [29] M. Verità, T. Toninato, A comparative analytical investigation on the origins of the Venetian glass making, *Riv. Stn. Sper. del vetro* 20 (4) (1990) 169–176.
- [30] A. Bouquillon, B. Barthélemy De Saizieu, A. Duval, Glazed steatite beads from Mergharh and Nausharo (Pakistani Balochistan), in: P. Vandiver, J.R. Druzik, J.L. Galvan Madrid, I.C. Freestone, G. Segan Wheeler (Eds.), *Materials Research Society Symposium Proceedings. Materials Issues in Art and Archaeology IV*, vol. 352, Materials Research Society, Pittsburgh, Pennsylvania, 1995, pp. 527–538.
- [31] R.H. Brill, Chemical analyses of some early Indian glasses, in: H.C. Bhardwaj (Ed.), *Archaeometry of Glass—Proceedings of the Archaeometry Session of the XIVth International Congress on Glass-1986*, Indian Ceramic Society, Calcutta, New Delhi, India, 1987, pp. 1–25 (part I).
- [32] L. Dussubieux, P. Robertshaw, M.D. Glascock, LA-ICP-MS analysis of African glass beads: laboratory inter-comparison with an emphasis on the impact of corrosion on data interpretation, *Int. J. Mass Spectrom.* 284 (2009) 152–161.
- [33] Ch. Lilyquist, R. Brill, *Studies in Early Egyptian Glass*, The Metropolitan Museum of Art, New York, 1993.
- [34] Y. Barkoudah, J. Henderson, Plant ashes from Syria and the manufacture of ancient glass: ethnographic and scientific aspects, *J. Glass Stud.* 48 (2006) 297–321.
- [35] J. Henderson, J. Evans, P. Bellintani, A.M. Bietti-Sestieri, Production, mixing and provenance of Late Bronze Age mixed alkali glasses from northern Italy: An isotopic approach, *J. Archaeol. Sci.* 55 (2015) 1–8.
- [36] Th. Rehren, Aspects of the production of cobalt-blue glass in Egypt, *Archaeometry* 43 (2001) 483–489.
- [37] Y. Abe, R. Harimoto, T. Kikugawa, K. Yazawa, A. Nishisaka, N. Kawai, S. Yoshimura, I. Nakai, Transition in the use of cobalt-blue colorant in the New Kingdom of Egypt, *J. Archaeol. Sci.* 39 (2012) 1793–1808.
- [38] A. Shortland, N. Rogers, K. Eremin, Trace element discriminants between Egyptian and Mesopotamian Late Bronze Age glasses, *J. Archaeol. Sci.* 34 (5) (2007) 781–789.